



Preparation and characterization of Mg-doped ZnO thin films by sol-gel method

Kai Huang^a, Zhen Tang^a, Li Zhang^a, Jiangyin Yu^a, Jianguo Lv^{b,*}, Xiansong Liu^c, Feng Liu^d

^a Department of Mathematics & Physics, Anhui University of Architecture, Hefei 230601, China

^b Department of Physics and Electronic Engineering, Hefei Normal University, Hefei 230601, China

^c School of Physics and Material Science, Anhui University, Hefei 230039, China

^d School of Mathematics and Physics, Anhui Polytechnic University, Wuhu 241000, China

ARTICLE INFO

Article history:

Received 22 June 2011

Received in revised form

20 November 2011

Accepted 3 December 2011

Available online 13 December 2011

Keywords:

Mg-doped ZnO

Sol-gel method

Surface topography

Optical properties

ABSTRACT

Undoped and Mg-doped ZnO thin films were deposited on Si(1 0 0) and quartz substrates by the sol-gel method. The thin films were annealed at 873 K for 60 min. Microstructure, surface topography and optical properties of the thin films have been measured by X-ray diffraction (XRD), atomic force microscope (AFM), UV-vis spectrophotometer, and fluorophotometer (FL), respectively. The XRD results show that the polycrystalline with hexagonal wurtzite structure are observed for the ZnO thin film with Mg:Zn = 0.0, 0.02, and 0.04, while a secondary phase of MgO is evolved for the thin film with Mg:Zn = 0.08. The ZnO:Mg-2% thin film exhibits high c-axis preferred orientation. AFM studies reveal that rms roughness of the thin films changes from 7.89 nm to 16.9 nm with increasing Mg concentrations. PL spectra show that the UV-violet emission band around 386–402 nm and the blue emission peak about 460 nm are observed. The optical band gap calculated from absorption spectra and the resistivity of the ZnO thin films increase with increasing Mg concentration. In addition, the effects of Mg concentrations on microstructure, surface topography, PL spectra and electrical properties are discussed.

Crown Copyright © 2011 Published by Elsevier B.V. All rights reserved.

1. Introduction

Zinc oxide (ZnO), a wide band gap (3.37 eV) and a large excitation binding energy of 60 meV semiconductor, has attracted much attention for possible applications in optoelectronic devices [1–3]. Zinc oxide (ZnO) has been successfully included in the photonics, optoelectronics, spintronics, and gas sensors applications [4–6].

Especially, ZnO can be alloyed with another high optical band gap II–VI compounds like magnesium oxide (MgO) to increase its band gap. ZnO:Mg is a semiconductor composed of two materials, zinc oxide and magnesium oxide, which can be easily controlled over a wide range of temperatures because the ionic radii of Mg²⁺ and Zn²⁺ are similar [7]. Improvements in ZnO:Mg dopant technology [8] have led to many new applications in electronics and optoelectronics [9].

Mg-doped ZnO thin films have been prepared using various methods, such as radio frequency (rf) magnetron sputtering [10,11], spray pyrolysis [12], pulsed laser deposition [13], chemical vapor deposition [14], electro-deposition [15], the sol-gel method technique [16]. It is also experimentally established that the structural and optical properties of these thin films are very sensitive to the deposition conditions [17]. Among these methods, the sol-gel method is an attractive one due to its simplicity and reproducibility.

In the present study, Mg-doped ZnO thin films were deposited on silicon and quartz substrates by sol-gel method. The influence of Mg concentration on microstructure, surface morphologies, optical properties and electrical properties of the thin films were investigated.

2. Experimental details

Ethylene glycol monomethyl ether and monoethanol amine were used as the solvent and stabilizing agent, respectively. The source for Mg doping was magnesium chloride (MgCl₂). Zinc acetate dihydrate and MgCl₂ were first dissolved in a mixture of ethylene glycol monomethyl ether and monoethanol amine at room temperature. The concentration of zinc acetate was 0.5 mol/L. The atomic ratios of Mg:Zn were 0, 0.02, 0.04, and 0.08 (these films were named as ZnO, ZnO:Mg-2%, ZnO:Mg-4%, and ZnO:Mg-8%, respectively). The molar ratio of monoethanol amine to zinc acetate was kept at 1:1. The solution was stirred at 333 K for 120 min using a magnetic stirrer to get a clear, homogeneous and transparent sol, which served as the coating sol after being kept for 1 day. Mg-doped ZnO thin film was deposited on Si(1 0 0) substrate and quartz substrates using the spin coating method with 3000 rpm for 30 s. After spin coating, the substrates were kept at 423 K for 10 min to evaporate the solvent in the film and this procedure was repeated 10 times. These as-coated films were annealed at 873 K for 60 min in air and then cooled down to RT.

* Corresponding author. Tel.: +86 551 3674132; fax: +86 551 3674131.

E-mail address: jglv@hftc.edu.cn (J. Lv).

Crystal structure of the thin films was investigated using X-ray diffractometry (XRD, MACM18XHF) with Cu K α radiation ($\lambda = 0.1540$ nm). Surface morphology of the thin films was measured by atom force microscopy (AFM, CSPM4000) operating in contact mode. Optical transmittance spectra of the thin films were measured by UV-Vis spectrometer (U-4100). Photoluminescence (PL) spectra were investigated at room temperature by fluorescence spectrometer (FL, F-4500) with a xenon lamp as the light source excited at 325 nm. The resistivity of the films was measured by an electrical resistance meter (KEITHLEY 651A) with Ag electrodes.

3. Results and discussion

Fig. 1 shows XRD patterns of Mg-doped ZnO thin films prepared on Si substrate with different Mg concentrations annealed at 873 K for 60 min. The XRD patterns indicate that the ZnO, ZnO:Mg-2%, ZnO:Mg-4% thin films possess a polycrystalline ZnO with the hexagonal wurtzite structure. It can be seen that the undoped ZnO thin film is polycrystalline structure without preferred orientation. While the ZnO:Mg-2% and ZnO:Mg-4% thin films exhibit preferential *c*-axis orientation. The presence of MgO (2 2 2), (2 0 0) and (4 0 0) diffraction peaks indicated that Mg segregates in the form of MgO in the ZnO thin film with Mg:Zn = 0.08. Phase separation of MgO and ZnO can be explained that Mg atoms are more active than Zn atoms and react with oxygen preferentially. The similar results of XRD of Mg-doped ZnO thin films are presented by Kaushal et al. [18].

Fig. 2 shows the surface morphologies of the ZnO thin films with different Mg doping concentrations. It can be seen that the surface

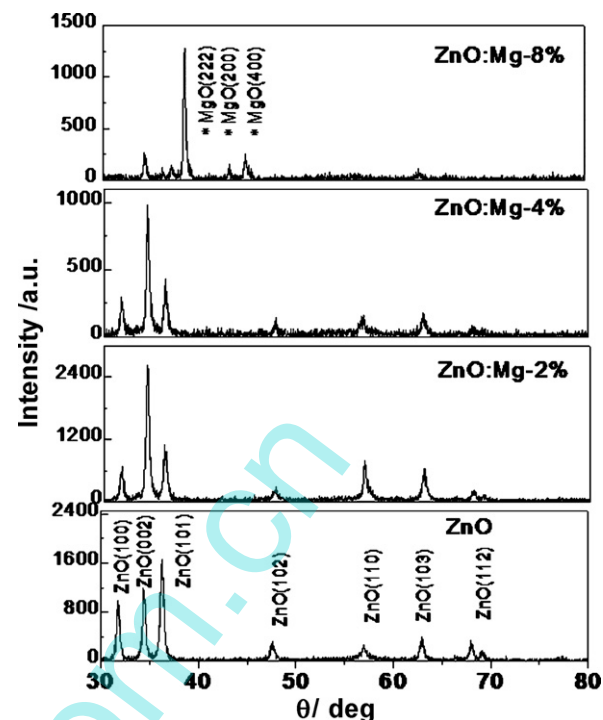


Fig. 1. XRD spectra of Mg-doped ZnO thin films annealed at 873 K for 60 min.

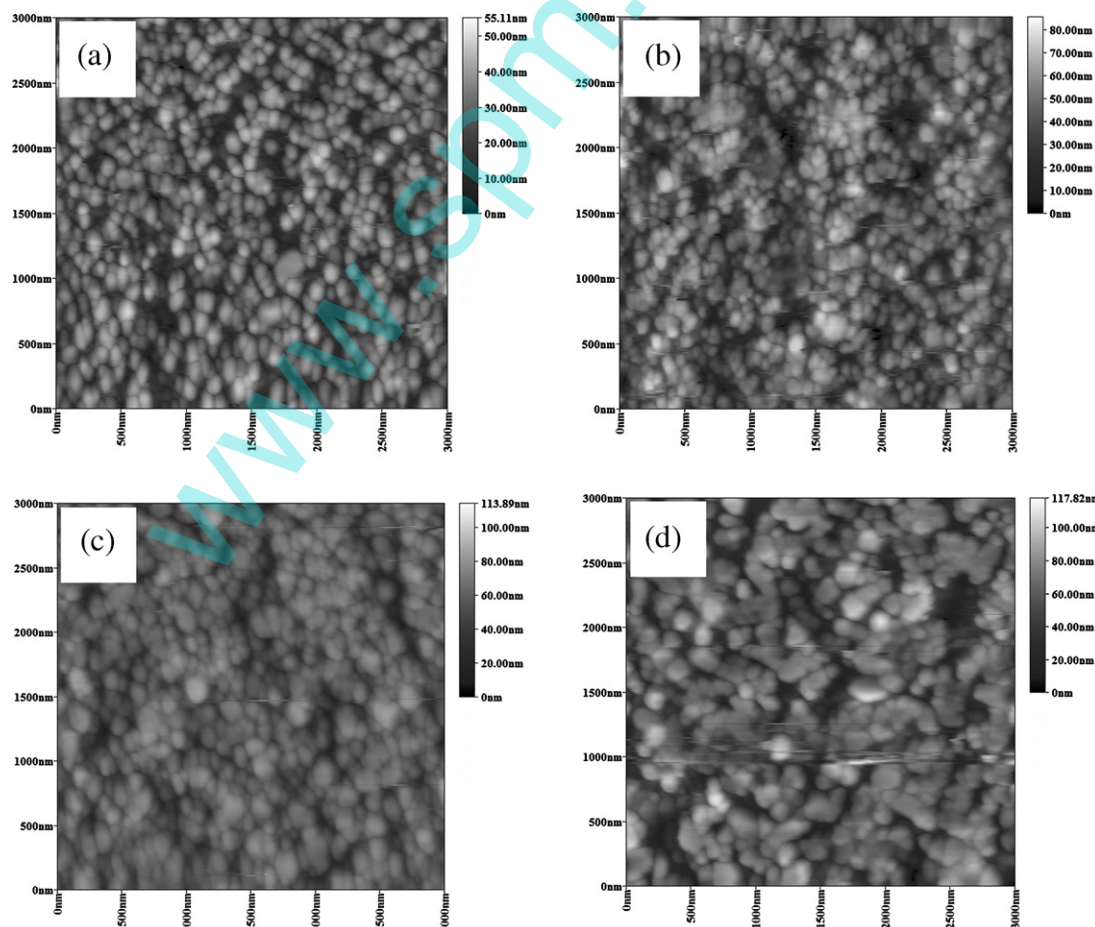


Fig. 2. Surface morphologies of (a) ZnO, (b) ZnO:Mg-2%, (c) ZnO:Mg-4% and (d) ZnO:Mg-8% Mg-doped ZnO thin films annealed at 873 K for 60 min.

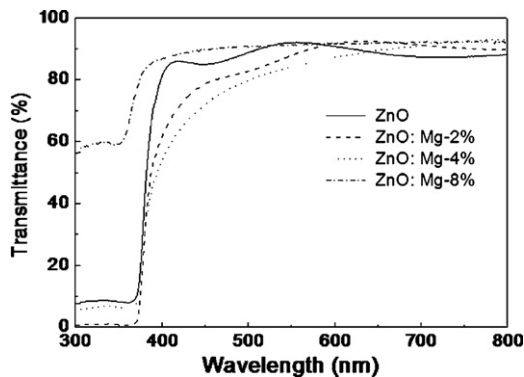


Fig. 3. Transmission spectra of Mg-doped ZnO thin films with different Mg concentrations annealed at 873 K for 60 min.

of the thin films consists of inhomogeneous nano-sized particles. The mean particle size increases with increasing of Mg concentration. The root-mean-square (rms) roughness of ZnO, ZnO:Mg-2%, ZnO:Mg-4%, ZnO:Mg-8% thin films are 7.89, 11.2, 12.3 and 16.9 nm, respectively. The rms roughness of the thin films increases with the doping which may be the result of the accumulation of the MgO particles on the surface of ZnO nano-grains. The similar results of surface morphologies of Mg-doped ZnO thin films are presented by Kumar et al. [19].

Fig. 3 shows the UV-vis transmission spectra of the Mg-doped ZnO thin films annealed at 873 K with different Mg concentrations. In this study, the absorbance of samples was measured as a function of wavelength in the range of 300–800 nm. It can be seen that all the thin films have an average optical transparency over 85% in the visible range and a sharp ultraviolet absorption edges.

The band gap is preferred to be evaluated from the optical transmission spectra. ZnO is a wide band gap semiconductor material with direct band gap. The optical band gap is given by Tauc relationship [20].

$$\alpha h\nu = A(h\nu - E_g)^n$$

where α is the absorption coefficient, A is the constant, h is the Planck's constant, ν is the photon frequency, E_g is the optical band gap and n is the 1/2 for direct band gap semiconductors. The functional relationships between $(\alpha h\nu)^2$ and photon energy $h\nu$ for undoped and Mg-doped ZnO films are shown in Fig. 4. Since $E_g = h\nu$

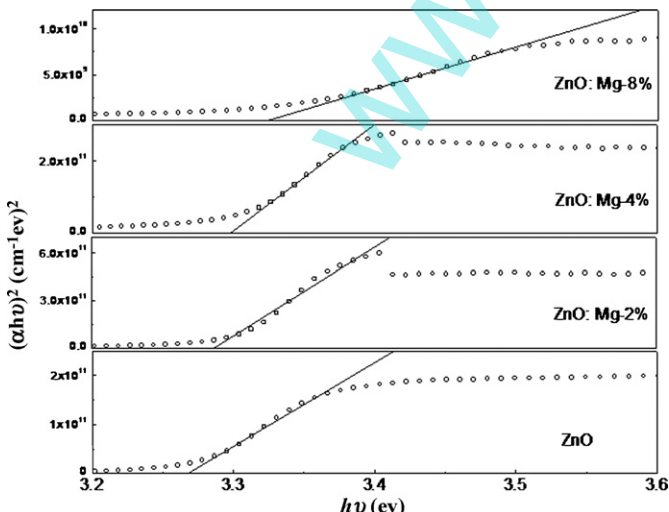


Fig. 4. The $(\alpha h\nu)^2$ versus $h\nu$ plots of Mg-doped ZnO thin films with different Mg concentrations annealed at 873 K for 60 min.

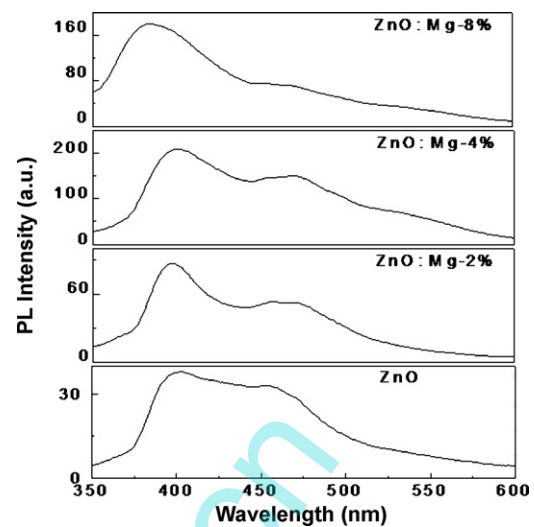


Fig. 5. Photoluminescence spectra of Mg-doped ZnO thin films with different Mg concentrations annealed at 873 K for 60 min.

when $(\alpha h\nu)^2 = 0$, an extrapolation of the linear region of the plot of $(\alpha h\nu)^2$ versus photo energy ($h\nu$) on the x -axis gives the value of the optical band gap E_g . The optical band gap calculated from absorption spectra of ZnO, ZnO:Mg-2%, ZnO:Mg-4%, and ZnO:Mg-8% thin films are 3.26, 3.29, 3.31 and 3.34 eV, respectively. The calculated results showed that the band gap of Mg-doped ZnO thin films were in the range 3.29–3.34 eV, larger than pure ZnO thin film. This may be attributed to the fact that new defects are introduced after Mg atoms substitute Zn atoms due to the electronegativity and ionic radius difference. Normally, ZnO is an n-type semiconductor, the Fermi level is inside the conduction band [21]. There are more electrons contributed by Mg dopant due to lower electron affinity of MgO compared to ZnO, which can be located at a higher Fermi level for the Mg-doped ZnO thin films. Thus the radiative recombination of these excitons may lead to a blueshift. The result is also in consistent with the reported results [22]. The increase in optical band with the Mg concentration, suggests that the ZnO:Mg thin film is a suitable material for potential optoelectronics in ZnO-based devices having a large band gap. The optical absorption at the absorption edge corresponds to the transition from valence band to the conduction band, while there is absorption in the energy region below 3.3 eV. The reason can be impurities or defects center in the Mg-doped ZnO thin films. Free excitons in semiconductor can be impurities or defects center in space constraints, the formation of so-called bound exciton. Therefore the absorption spectrum of energy is slightly lower than the free exciton absorption spectrum.

Fig. 5 shows the room-temperature PL of the Mg-doped ZnO thin films for various Mg concentrations annealed at 873 K for 60 min. Photoluminescence spectrum provides information on the optically active defects and relaxation pathways of excited states. It can be seen that a strong ultraviolet (384–402 nm) emission and a relatively weak blue emission (~460 nm) peak. It was well known that the UV emission peak usually originated from a near-band-edge (NBE) transition of the wide band gap due to the annihilation of excitons [23]. The results show that as Mg concentration increases, intensity of the ultraviolet emission bands increase to the maximum when Mg:Zn atomic ratio is 0.04, and then decrease. At the same time, the ultraviolet emission peak blueshifts from 402 nm to 384 nm, because of the modulation of the band-gap caused by Mg substitution, which suggests that the optical band gap of the Mg-doped ZnO thin films can be tunable by changing the Mg concentrations. The magnitude of the blueshift of the PL peak is much larger than that of the band-gap widening, probably due to the

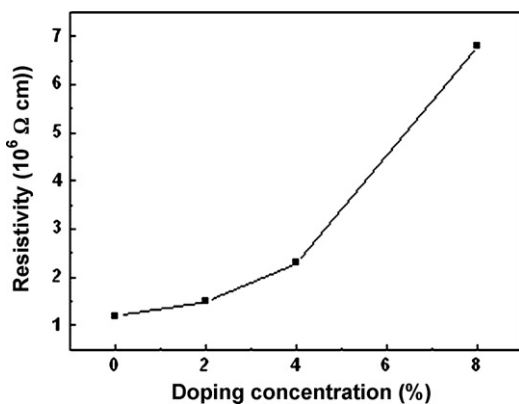


Fig. 6. Resistivities of Mg-doped ZnO thin films with different Mg concentrations annealed at 873 K for 60 min.

influence by impurities, defects, and strong surface recombination under high-energy excitation [24]. The blue emission observed at 460 nm may be attributed to the exciton recombination between the electron localized at the interstitial zinc (Zn_i) and the holes in the valence band [25].

Fig. 6 shows the resistivities of the ZnO thin films with different Mg doping concentrations. It is clear that the resistivity of the ZnO thin films increases with increasing of Mg concentration. As we know that the valences of Zn^{2+} and Mg^{2+} are the same, and the substitution of Mg^{2+} for the group II cation of Zn should not generate or consume carriers of ZnO. However, electrical properties of the ZnO thin films change after Mg doping. This presumably results from the substitution of Mg ions with a smaller ionic radius for Zn sites [26]. The positions of the (0 0 2) diffraction peak change based on the XRD results, which results in lattice distortion to some extent. This would increase the resistivity of ZnO thin films. On the other hand, there is also the possibility that a spot of Mg at the grain boundaries may produce electrical barriers, increasing scattering of the carriers, and thus increase the resistivity. As a result, the resistivity of the ZnO thin films increases after Mg is doped.

4. Conclusion

Undoped and Mg-doped ZnO thin films were deposited on Si(1 0 0) and quartz substrates using the sol-gel process. The XRD patterns indicate that the ZnO, ZnO:Mg-2%, ZnO:Mg-4% thin films possess a polycrystalline ZnO with the hexagonal wurtzite structure. While the ZnO:Mg-2% and ZnO:Mg-4% thin films exhibit preferential *c*-axis orientation. As Mg:Zn atomic ratio is 0.08, Mg segregates in the form of MgO. AFM analysis revealed that rms roughness of ZnO thin films increases with increasing Mg

concentrations annealed at 873 K. Transmittance of the thin films is over 85% in the visible region. The optical band gap increases from 3.26 eV to 3.34 eV with increasing Mg concentration. PL spectra were investigated at room temperature. We can observe the strong ultraviolet (384–402 nm) emission and the weak blue emission (~460 nm) peaks. The ultraviolet emission peaks blueshifts with increasing Mg doping concentration. On the other hand, the resistivities of the ZnO films are enhanced by Mg introduction and increase with increasing doping concentrations. These may be caused by the lattice distortion in the films and the electrical barriers by the Mg deposited at the grain boundaries.

Acknowledgements

This work was supported by National Natural Science Foundation of China (nos. 51072002, 11104001, 51102072, 51002156) and Natural Science Foundation of Anhui Higher Education Institution of China (nos. KJ2010A284, KJ2010B024 and KJ2010B172) and Foundation of Quality Project of Hefei Normal University (no. 2010yj27).

References

- [1] J. Liu, H. Xia, D. Xue, L. Lu, *J. Am. Chem. Soc.* 131 (2009) 12086.
- [2] C. Yan, D. Xue, *Adv. Mater.* 20 (2008) 1055.
- [3] H. Xia, W. Xiao, M.O. Lai, L. Lu, *Funct. Mater. Lett.* 2 (2009) 13.
- [4] T.H. Fang, S.H. Kang, *J. Phys. D: Appl. Phys.* 41 (2008) 245303.
- [5] Anna Og, Dikovska, P.A. Atanasov, A.Ts. Andreev, B.S. Zafirova, E.I. Karakoleva, T.R. Stoyanchov, *Appl. Surf. Sci.* 254 (2007) 1087.
- [6] D.X. Jiang, L. Cao, W. Liu, G. Su, H. Qu, Y.G. Sun, B.H. Dong, *Nanoscale Res. Lett.* 4 (2009) 78.
- [7] D.K. Hwang, M.C. Jeong, J.M. Myoung, *Appl. Surf. Sci.* 225 (2004) 217.
- [8] H.C. Hsu, C.Y. Wu, H.M. Cheng, W.F. Hsieh, *Appl. Phys. Lett.* 89 (2006) 13101.
- [9] T.H. Fang, S.H. Kang, *J. Appl. Phys.* 105 (2009) 113512.
- [10] P. Wang, N. Chen, Z. Yin, R. Dai, Y. Bai, *Appl. Phys. Lett.* 89 (2006) 202102.
- [11] M.K. Jayaraj, *Bull. Mater. Sci.* 25 (2002) 227.
- [12] P.P. Sahay, S. Tewari, R.K. Nath, *Cryst. Res. Technol.* 42 (2007) 723.
- [13] E. Bellingeri, D. Marre, I. Pallecchi, L. Pellegrino, G. Canu, A.S. Siri, *Thin Solid Films* 486 (2005) 186.
- [14] C.W. Lin, T.Y. Cheng, L. Chang, J.Y. Juang, *Phys. Stat. Sol. (c)* 1 (2004) 851.
- [15] M. Fahoume, O. Maghfoul, M. Aggour, B. Hartiti, F. Chraibi, A. Ennaoui, *Sol. Energy Mater. Sol. Cells* 90 (2006) 1437.
- [16] G. Srinivasan, J. Kumar, *Cryst. Res. Technol.* 41 (2006) 893.
- [17] K. Yoshino, T. Hata, T. Kakeno, H. Komaki, M. Yoneta, Y. Akaki, T. Ikari, *Phys. Stat. Sol. (c)* 2 (2003) 626.
- [18] A. Kaushal, D. Kaur, *Solar Energy Mater. Sol. Cells* 93 (2009) 193.
- [19] S. Kumar, V. Gupte, K. Sreenivas, *J. Phys. Condensed Matter* 18 (2006) 3343.
- [20] M. Girtan, G. Folcher, *Surf. Coat. Technol.* 172 (2003) 242.
- [21] S. Suwanboon, P. Amornpitoksuk, A. Sukolrat, *Ceram. Int.* 37 (2011) 1359.
- [22] J. Narayan, A.K. Sharma, A. Kvit, C. Jin, J.F. Muth, O.W. Holland, *Solid State Commun.* 121 (2002) 9.
- [23] J. Bang, H. Yang, P.H. Holloway, *Nanotechnology* 17 (2006) 973.
- [24] S. Fujita, H. Tanaka, S. Fujita, *Cryst. Growth J.* 278 (2005) 264–267.
- [25] B. Kumar, H. Gong, S. Vicknesh, S.J. Chua, S. Tripathy, *Appl. Phys. Lett.* 89 (2006) 071922.
- [26] J.P. Han, A.M.R. Senos, P.Q. Mantas, *J. Eur. Ceram. Soc.* 22 (2002) 1653.